RATIONAL APPROXIMATION OF P-WAVE KINEMATICS – PART 1: TRANSVERSELY ISOTROPIC MEDIA[1]

Mohammad Mahdi Abedi

Basque Center for Applied Mathematics, Bilbao, Spain. formerly at University of Tehran, Institute of Geophysics, Tehran, Iran.

E-mail: mabedi@bcamath.org

ABSTRACT

In seismic data processing and several wave propagation modeling algorithms, the phase velocity, group velocity, and traveltime equations are essential. To have these equations in explicit form, or to reduce algebraic complexity, approximation methods are used. For the approximation of P-wave kinematics in acoustic transversely isotropic media, we propose a new flexible 2D functional equation in a continued fraction form. Using different orders of the continued fraction, we obtain different approximations for (1) phase velocity as a function of phase direction, (2) group velocity as a function of group direction, and (3) traveltime as a function of offset. We also obtain approximations of group direction as a function of phase direction, and phase direction as a function of group direction. The proposed approximations have a rational form, which is considered as being algebraically simple and computationally efficient. The employed continued fraction form rapidly converges to exact kinematics. By introducing the optimal ray into our approximations and using it for parameter definition, the convergence becomes faster, so the accuracy of the existing most accurate approximations is available by the third order, and new most accurate approximations are obtained by the fourth order of the proposed general form. The error of the most accurate version of the proposed approximations is below 0.001% for moderate anisotropic models with an anellipticity parameter up to 0.3. This high accuracy is considered to be attractive in practical implementations that use the kinematical equations and their derivatives.
Keywords: Anisotropy, Acoustic properties, Traveltime, Phase, 2D

[1] This paper is published by GEOPHYSICS: DOI: 10.1190/geo2020-0005.1

INTRODUCTION

The effect of anisotropy on wave propagation has been widely recognized in modern seismic studies. A transversely isotropic (TI) symmetry is one of the simplest anisotropic models that has been employed in many practical applications. The popularity of TI anisotropy is due to its ability to describe the observed variation of velocity with angle, in 2D models. The pseudo acoustic assumption (Alkhalifah, 1998) presents a simplified TI anisotropy (compared to the elastic case) for the description of P-wave propagation kinematics.

Anisotropy results in a variation of velocity with direction, and different definitions of velocity within the phase and group domains. To use TI models in seismic studies, explicit equations of velocity as a function of direction are required, in both the phase and group domains. In the phase domain, such an equation is readily calculated from the Christoffel equation; therefore, the only purpose of proposing an approximate equation is for algebraic simplicity. In the group domain, the exact equation exists only in a parametric form; therefore, besides the algebraic simplicity, the required explicit form of the group velocity as a function of group angle is the reason that we need an approximate equation. This has led to much research being devoted to the development of new group velocity (or moveout approximation) for TI media (Tsvankin and Thomsen, 1994; Alkhalifah and Tsvankin, 1995; Alkhalifah 2000, 2011; Fomel, 2004; Ursin and Stovas, 2006; Aleixo and Schleicher, 2010; Xu et al., 2017; Abedi and Stovas, 2019a), and for more general 2D media (Fomel and Stovas, 2010; Stovas and Fomel, 2017; Ravve and Koren, 2017; Stovas and Fomel, 2019; Abedi and Stovas, 2019b).

Applications of a phase-velocity approximation include ray tracing (Alashloo, and Ghosh, 2018), wavefield modeling (Fomel et al., 2013), and phase-shift migration (Ristow, 1998). Group velocity approximations have application in ray tracing, seismic tomography (Eaton, 1993), and model parameter estimation (Pšenčík el al., 2018). A moveout equation is connected to group velocity, therefore, they have common applications. Moveout approximations are used in many basic data processing steps, such as normal moveout correction (e.g. Abedi et al., 2019a), calculation of Green's function for migration, and Radon transform (e.g. Abedi et al., 2019b). Moreover, equations for the conversion of phase to group direction, and vice versa are useful in ray tracing.

In practice, an approximation should be simple because the algebraic complexity of an equation can significantly affect the computational cost. Rational equations have polynomials in their numerator and denominator; therefore, they are considered as being algebraically simple and computationally fast. An attempt on rationalization of traveltime approximations is proposed by Song et al. (2016) using the Padé expansion, but the result remains algebraically complicated.

In this study, we propose explicit rational equations for the approximation of phase velocity, group velocity, traveltime, and the conversion between the phase and group directions in acoustic TI media. We explain a robust method for parameter definition of our approximations. Then compare the accuracy of the proposed approximations with classical and recent approximations.

THEORY

A common approach for the approximation of P-wave kinematics in TI media is to assume an elliptical background, and add a perturbation that approximates the anellipticity effect. A basic rational form of this kind of approximation is proposed by Muir and Dellinger (1985). Their approximations for phase velocity squared (v^2) reads,

$$v^2(\mathbf{n}) \simeq e + \frac{Ab}{e}, \tag{1}$$

where, $e(\mathbf{n}) = n_1^2 v_1^2 + n_3^2 v_3^2$ is the elliptical part, and $b(\mathbf{n}) = n_1^2 n_3^2 v_1^2 v_3^2$ is a 2D cross-term. Parameter A defines the anelliptical intensity, and v_1, and v_3 are the horizontal and vertical (axial) velocities, respectively (using Thomsen (1986) notation, $v_1 = v_3\sqrt{1+2\varepsilon}$). The $\mathbf{n} = (\sin\theta, \cos\theta)$ is the phase direction vector, where θ is the phase angle from the vertical axis.

In the group domain, the Muir and Dellinger (1985) approximation for the inverse of group velocity squared (V^{-2}) has the same functional form of equation 1:

$$V^{-2}(\mathbf{N}) \simeq \hat{e} + \frac{\hat{A}\hat{b}}{\hat{e}}, \tag{2}$$

where $\hat{e}(\mathbf{N}) = N_1^2/v_1^2 + N_3^2/v_3^2$, and $\hat{b}(\mathbf{N}) = (N_1^2 N_3^2)/(v_1^2 v_3^2)$ are the elliptical and cross-term parts. The parameter $\hat{A}$ defines the anelliptical intensity; and $\mathbf{N} = (\sin\Theta, \cos\Theta)$ is the group direction vector, where Θ is the group angle from the vertical axis.

The accuracy of approximations in equations 1 and 2 is insufficient for practical purposes but can be used as a basis for developing more accurate approximations. In this study, we expand the Muir and Dellinger (1985) functional form in a generalized continued fraction to obtain a general flexible form for kinematics approximations in both phase and group domains, as follows.

Phase velocity

Using a continued-fraction expansion of the phase velocity approximation in equation 1, we obtain the following phase velocity approximation in acoustic VTI media,

$$v^2(\mathbf{n}) \simeq e + \cfrac{Ab}{e + \cfrac{Bb}{e + \cfrac{Cb}{e}}}, \tag{3}$$

where $e(\mathbf{n})$ and $b(\mathbf{n})$ are the elliptical and cross-term parts, and A, B, C, are the equation parameters, dependent on the anellipticity parameter (η). Different orders of equation 3 (determined by the number of fractions in equation 3) present different examples of approximations. A higher order of the approximation means a higher the degree of freedom in fitting it to the exact equation, but also a higher algebraic complexity.

First, using the second-order of equation 3, the parameters of our simplest rational phase-velocity approximation are calculated as,

$$\begin{aligned} A &= -2\eta/(1+2\eta), \\ B &= -2+2/\sqrt{1+2\eta}, \\ C &= 0. \end{aligned} \tag{4}$$

The parameter A is obtained by fitting the second derivative of equation 3 to its exact value along the vertical direction in acoustic TI media (i.e., equating the second term of the series expansions in equation A-1 to that in equation A-4). Equating a term of the series expansion of equation 3 along vertical, the equivalent term of the series along the horizontal is automatically matched to the exact term. This is the result of an internal symmetry that exists in all kinematical properties in TI media, and is preserved in our proposed form of approximations. This symmetry is in a way that an interchange of horizontal and vertical velocities only flips the slowness surface (or other kinematical properties). This can be seen by comparing different orders of Taylor series for any kinematical properties at the vertical and horizontal directions (Appendix A).

To define the parameter B as is given in equation 3, we have changed the fitting location. Finding B by fitting equation 3 to the exact phase velocity at any direction close to vertical, the approximation is also fitted to a corresponding direction near the horizontal (dual fits that are resulted from the aforementioned symmetry, and are explained in Appendix B). Going further away from the axes, these two fitting directions move nearer until at a specific direction they meet (Appendix B). This direction is called the direction of optimal ray and is introduced by Abedi and Stovas (2019a) and Abedi et al. (2019c) for their approximations in the group domain. Properties and direction of the optimal ray are calculated in Appendix B. Finding a parameter of any of our approximations at the optimal ray, the two fits in which this parameter results will be at the same point but for derivatives of different orders. The second-order phase velocity approximation (equation 3 with parameters given in equation 4) has six fits to exact phase velocity, two fits through v_1 and v_3, and four fits through A and B (Table 1).

Next, to have a more accurate approximation, we use the third-order of equation 3 and obtain the parameters as,

$$
\begin{aligned}
A &= -2\eta/(1+2\eta), \\
B &= A, \\
C &= -2+2/\sqrt{1+2\eta}.
\end{aligned}
\tag{5}
$$

In equation 5, the parameter C is found in the optimal direction. The third-order phase velocity approximation (equation 3 with parameters given in equation 5) has eight fits to exact phase velocity, two fits through v_1 and v_3, and six fits through A, B, and C parameters (Table 1). Figure 1 shows the relative accuracy of the second and third-order of the proposed approximation in a model with $\eta = 0.3$. Both of the proposed approximations are highly accurate with smooth errors, but the third-order approximation is more accurate due to the extra fits to the exact phase velocity derivatives at 0 and 90° angles.

Comment

Expanding the continued fraction in equation 3 to infinite order, and defining all the anelliptic parameters (coefficient of the cross-term b) from different orders of derivatives at vertical and horizontal directions, a familiar closed form is obtained. The closed-form is the exact phase velocity equation in acoustic TI media,

$$
v^2(\mathbf{n}) = e + \cfrac{Ab}{e + \cfrac{Ab}{e + \ddots}} = \frac{e}{2} + \sqrt{\left(\frac{e}{2}\right)^2 + Ab}, \tag{6}
$$

where $A = -2\eta/(1+2\eta)$. The expansion in equation 6 rapidly converges so that the fourth-order fraction has a maximum relative error of less than 0.001% for $\eta = 0.3$. Using the optimal ray and the modified parameter definition in equation 5, we make the convergence faster so that we reach the accuracy of the fourth-order with the third-order fraction. The truncation of the expansion in equation 6 and application of the optimal ray can be done at any order; doing so, all parameters equal to A, except for highest order parameter which equals to the C in equation 5.

Group velocity

Using a similar continued fraction form in the group domain, we obtain the following group velocity approximation in acoustic VTI media,

$$V^{-2}(\mathbf{N}) \simeq \hat{e} + \cfrac{\hat{A}\hat{b}}{\hat{e} + \cfrac{\hat{B}\hat{b}}{\hat{e} + \cfrac{\hat{C}\hat{b}}{\hat{e} + \cfrac{\hat{D}\hat{b}}{\hat{e}}}}}, \tag{7}$$

where $\hat{e}(\mathbf{N})$ and $\hat{b}(\mathbf{N})$ are the elliptical and cross-term parts that are introduced in equation 2, and $\hat{A}, \hat{B}, \hat{C}, \hat{D}$ are the equation parameters (the superscript ^ is used to distinguish the parameters in the group domain).

First, using the second-order of the proposed functional form, the parameters of our simplest group velocity approximation, are obtained as,

$$\begin{aligned} \hat{A} &= 2\eta, \\ \hat{B} &= 2\left(\eta - 1 + \sqrt{1+2\eta}\right), \\ \hat{C} &= \hat{D} = 0. \end{aligned} \tag{8}$$

Similar to the phase velocity approximation, the parameter $\hat{A}$ is obtained by fitting the second derivatives of equation 7 to their exact values along both the vertical and horizontal directions in acoustic VTI media, and $\hat{B}$ is obtained from fitting equation 7 to the exact group velocity (equation B-6) along the optimal group direction (equation B-4). The proposed second-order approximation has six fits to the exact group velocity, as presented in Table 1.

We obtain our second, more accurate, group velocity approximation by using the third-order of equation 7. The parameters of the third-order approximation are obtained as,

$$\begin{aligned} \hat{A} &= 2\eta, \\ \hat{B} &= 4\left(\eta + \eta^2\right), \\ \hat{C} &= 4\frac{2\eta - 1 + (1+2\eta)^{3/2}}{3 + \sqrt{1+2\eta}}, \\ \hat{D} &= 0. \end{aligned} \tag{9}$$

The third-order group velocity approximation has eight fits to exact group velocity along three directions, as presented in Table 1.

Using the fourth-order of equation 7, the parameters of our most accurate group velocity approximation are obtained as,

$$\hat{A} = 2\eta,$$
$$\hat{B} = 4\left(\eta + \eta^2\right),$$
$$\hat{C} = \left(4 + \hat{D}\right)\frac{2\eta - 1 + \left(1 + 2\eta\right)^{3/2}}{3 + \sqrt{1 + 2\eta}}, \tag{10}$$
$$\hat{D} = 4 - 2\frac{13 - 2\eta + \left(7 + 2\eta\right)\sqrt{1 + 2\eta}}{\left(1 + \eta\right)\left(5 + 2\eta + 5\sqrt{1 + 2\eta}\right)}.$$

In equation 10, the parameters $\hat{C}$ and $\hat{D}$ are found from the exact velocity and its derivatives of different orders at the optimal group direction (Appendix B). The fourth-order approximation has ten fits to the exact group velocity and its derivatives along three directions, as presented in Table 1.

The relative accuracy of the proposed group velocity approximations is shown in Figure 2. The relative errors of the proposed approximations are smooth and reach zero at vertical, horizontal, and optimal directions. For comparison, the Sripanich and Fomel (2015), and Abedi et al. (2019c) approximations are also included in Figure 2. Abedi et al. (2019c) use the optimal direction for parameter definition in the Stovas and Fomel (2019) equation. Being more accurate than Abedi et al. (2019c), the proposed fourth-order rational approximation is the most accurate approximation for group velocity in VTI media.

Traveltime

A group velocity approximation can be converted to a reflection traveltime (moveout) approximation, using simple geometrical equations. Converting our proposed group velocity (equation 7) to a moveout approximation, we obtain,

$$t^2\left(x\right) \simeq h + \cfrac{\hat{A}\tau}{h + \cfrac{\hat{B}\tau}{h + \cfrac{\hat{C}\tau}{h + \cfrac{\hat{D}\tau}{h}}}}, \tag{11}$$

where $h\left(x\right) = t_0^2 + x^2/v_1^2$ is the hyperbolic part, $\tau\left(x\right) = t_0^2 x^2/v_1^2$ is the cross-term, t_0 is zero-offset two-way time, x is offset, v_1 is the horizontal velocity ($v_1 = v_{nmo}\sqrt{1+2\eta}$), and $\hat{A}, \hat{B}, \hat{C}, \hat{D}$ are defined the same as for the group velocity. The second-, third-, and fourth-order traveltime approximations are obtained by employing equations 8, 9, and 10 for the definition of parameters in equation 11, respectively. As shown in Table 1, different orders of the proposed approximation have different fits to exact traveltime and its derivatives around zero, optimal, and infinite offsets (asymptote).

The second-order of the proposed traveltime approximation has similar algebraic complexity as the famous rational moveout approximation (Tsvankin and Thomsen, 1994; Alkhalifah and Tsvankin, 1995), but as Figure 3 shows has higher accuracy. The relative error of the fourth-order approximation is smooth and less than 0.001% for $\eta = 0.3$ (Figure 3), which makes it the most accurate moveout approximation for this model.

Phase and group directions

The exact relations for the phase to group, and group to phase velocity conversion are given in Dellinger and Muir (1985), and Stovas et al. (2018). Based on those relations, the proposed phase and group velocity approximations can be used to derive the equation of group direction as a function of phase directions, and vice versa. First, we present the equation of the group direction (**N**) as a function of phase direction (**n**) as,

$$N_1^2(\mathbf{n}) = \frac{\left(n_3^2 d + 2n_1 v^2\right)^2}{n_3^2 d^2 + 4v^4}, \tag{12}$$

where $v^2(\mathbf{n})$ is the phase velocity squared given in equation 2, and d is its derivative with respect to n_1 which we approximate as,

$$d = 2n_1 \frac{A\left(n_1^2 - n_3^2\right)v_1^2 v_3^2 - \left(v_1^2 - v_3^2\right)v^2}{e - 2v^2}. \tag{13}$$

We have $N_1 = \sin\Theta$, $N_3^2 = 1 - N_1^2$, and all other terms are defined the same as presented in the phase velocity section. The proposed relation in equation 13 is a rationalized approximation of the exact equation. We use the exact conversion equation and replace the square root terms with the proposed rational approximation for phase velocity squared. Doing so, we obtain a more accurate relation in equation 13 than directly using the derivative of equation 2.

Next, we present the equation of phase direction (**n**) as a function of group direction (**N**) as,

$$n_1^2(\mathbf{N}) = \frac{\left(N_3^2 \hat{d} + 2N_1 V^{-2}\right)^2}{N_3^2 \hat{d}^2 + 4V^{-4}}, \tag{14}$$

where $n_1 = \sin\theta$, $n_3^2 = 1 - n_1^2$, the inverse of group velocity squared ($V^{-2}(\mathbf{N})$) is given in equation 7, and $\hat{d}$ is its derivative with respect to N_1. For the second-order of equation 7, $\hat{d}$ is obtained as,

$$\hat{d} \simeq \hat{A}\hat{b}\,\frac{2\hat{e}^3\left(N_3^2-N_1^2\right)+\hat{g}\left(\hat{b}\hat{B}-\hat{e}^2\right)N_1N_3^2}{\left(\hat{b}\hat{B}+\hat{e}^2\right)^2 N_1N_3^2}+\hat{g}, \tag{15}$$

where $\hat{g}=2N_1\left(v_1^{-2}-v_3^{-2}\right)$, and all other terms are defined the same as presented in the group velocity section. For the third-order of equation 7, $\hat{d}$ is calculated as

$$\hat{d} \simeq 2\hat{A}\hat{b}\left(N_1^2-N_3^2\right)\frac{\hat{b}\left(\hat{e}^2+\hat{w}\right)\hat{B}-\hat{w}^2}{\hat{e}N_1N_3^2\hat{w}^2}+\hat{A}\hat{b}\hat{g}\,\frac{\hat{b}\left(2\hat{e}^2+\hat{w}\right)\hat{B}-\hat{w}^2}{\hat{e}^2\hat{w}^2}+\hat{g}, \tag{16}$$

where $\hat{w}=\hat{b}\left(\hat{B}+\hat{C}\right)+\hat{e}^2$. Note that the calculated equations of phase-to-group, and group-to-phase direction conversions have rational form.

Figure 4 shows the accuracy of the phase-to-group, and group-to-phase angle conversion using the proposed approximations. In Figure 4 the error is defined as the difference between the exact and approximated angles. In equations 12 and 14, the kinematic properties and their derivatives of the first order are used; therefore, in Figure 4 the conversion is exact at the vertical, horizontal, and optimal directions, which are the fitting directions in our approximations. Based on Figure 4, the maximum error of using the third-order of equation 3 in equation 12 is 0.00025°, and the maximum error of using the fourth-order of equation 7 in equation 14 is 0.0024°.

Ray-traced parameterization

In the previous parts, the parameters of the proposed equations are derived for acoustic VTI media. In this part, we present the general definition of parameters, by using the properties of one mid-angle (or mid-offset) ray to define the parameters. The ray-based parameter definition extends the potential application of the proposed approximations to more general 2D models, such as 2D sections of anisotropic media with lower symmetries. Here, we use each kinematic properties and their first-order derivatives at one mid-angle ray to define the anelliptic parameters in equation 3, 7, and 11. For equation 3 we obtain,

$$\begin{aligned} A &= -\frac{\left(\bar{n}_1^2v_1^2+\bar{n}_3^2v_3^2-\bar{v}^2\right)^2\left(\bar{n}_1^4v_1^4-\bar{n}_3^4v_3^4\right)}{\bar{n}_1^3\bar{n}_3^4v_1^2v_3^2\bar{v}\left(\left(\bar{n}_1^2v_1^2+\bar{n}_3^4v_3^2\right)\bar{v}'+\bar{n}_1\left(v_3^2-v_1^2\right)\bar{v}\right)}, \\ B &= \left(\frac{\bar{v}^2}{\bar{v}^2-\bar{n}_1^2v_1^2-\bar{n}_3^2v_3^2}-1\right)A-\frac{\left(\bar{n}_1^2v_1^2+\bar{n}_3^2v_3^2\right)^2}{\bar{n}_1^2\bar{n}_3^2v_1^2v_3^2}, \end{aligned} \tag{17}$$

where $\bar{v}$ is the exact phase velocity, and $\bar{v}'$ is its derivative with respect to angle at a reference mid-angle phase direction $\bar{\mathbf{n}}=\left(\bar{n}_1,\bar{n}_3\right)$. For equation 7 we calculate,

$$\hat{A} = \frac{\left(\bar{N}_1^2 + \bar{N}_3^2\right)\left(\bar{N}_3^2\bar{V}^2 v_1^2 + \left(\bar{N}_1^2\bar{V}^2 - v_1^2\right)v_3^2\right)^2\left(\bar{N}_1^4 v_3^4 - \bar{N}_3^4 v_1^4\right)}{\bar{N}_1^3\bar{N}_3^4 v_1^4 v_3^4 \bar{V}^2\left(v_3^2 - v_1^2 + \bar{V}^5 V'\left(\bar{N}_3^2 v_1^2 + \bar{N}_1^2 v_3^2\right)\right)},$$
$$\hat{B} = \left(\frac{v_1^2 v_3^2}{v_1^2 v_3^2 - \bar{V}^2\left(\bar{N}_3^2 v_1^2 + \bar{N}_1^2 v_3^2\right)} - 1\right)\hat{A} - \frac{\left(\bar{N}_3^2 v_1^2 + \bar{N}_1^2 v_3^2\right)^2}{\bar{N}_1^2\bar{N}_3^2 v_1^2 v_3^2}, \tag{18}$$

where $\bar{V}$ is the exact group velocity, and V' is its derivative with respect to group angle at a reference group direction $\bar{\mathbf{N}} = \left(\bar{N}_1, \bar{N}_3\right)$. For the traveltime approximation in equation 11, we obtain,

$$\hat{A} = -\frac{\left(\left(t_0^2 - \bar{t}^2\right)v_1^2 + \bar{x}^2\right)^2\left(t_0^4 v_1^4 - \bar{x}^4\right)}{t_0^2 v_1^4 \bar{x}^3\bar{t}\left(\bar{x}\bar{t} - \bar{p}\left(t_0^2 v_1^2 + \bar{x}^2\right)\right)},$$
$$\hat{B} = \left(\frac{\bar{t}^2 v_1^2}{\left(\bar{t}^2 - t_0^2\right)v_1^2 - \bar{x}^2} - 1\right)\hat{A} - \frac{\left(t_0^2 v_1^2 + \bar{x}^2\right)^2}{t_0^2 v_1^2 \bar{x}^2}, \tag{19}$$

where $\bar{t}$ is the exact traveltime, and $\bar{p}$ is its derivative with respect to offset (ray parameter) at an arbitrary finite reference offset $\bar{x}$. The general parameters definitions presented in equations 17-19 do not give two fits through each parameter because the previously mentioned internal symmetry, which is the reason for the dual fits, is limited to homogeneous acoustic TI media.

NUMERICAL ANALYSIS

To more comprehensively study the accuracy of the proposed approximations, we use multiple models that vary by their anellipticity parameter within the range $\eta \in [-0.2, 0.6]$. In acoustic TI media, the parameter η has no theoretical bonds, and the selected range is based on empirical observations of strongly anisotropic models. We evaluate the maximum relative errors of each equation when compared with the exact kinematics in acoustic VTI media, using the aforementioned models. As is shown in Appendix B, the magnitudes of the maximum relative errors of the proposed equations are independent of the elliptical background because of the normalization, therefore, the only influencing model parameter is η.

Figure 5a compares the maximum magnitude of relative errors of the second and third-order rational phase velocity approximations with Muir and Dellinger (1985). The Muir and Dellinger (1985) approximation equals to the first order of our approximation. Therefore, the higher accuracy of our third-order approximation compared to the second-order, and that compared to the first-order approximation remains valid in all models.

A comparison of different group velocity approximations is shown in Figure 5b. The proposed approximations are compared with recent approximations proposed by Sripanich and Fomel (2015) and Abedi et al. (2019c). The higher the magnitude of η, the higher the relative errors will be. Figure 5b shows that the loss of accuracy with η increment has a higher rate for the proposed rational approximations than for Abedi et al. (2019c). Accordingly, the error of our third-order rational group velocity approximation surpasses that of Abedi et al. (2019c) around $\eta = 0.25$. Figure 5b shows that the fourth-order rational approximation remains the most accurate approximation in all the models. Comparing Figure 5a and 5b, the proposed approximations in the phase and group domain approximately reach the same level of accuracy when the group approximation use one higher order of the continued fraction.

A similar comparison of the maximum relative errors of different traveltime approximations is shown in Figure 5c. We choose to compare our rational approximations with the Alkhalifah and Tsvankin (1995), and the Fomel and Stovas (2010) moveout approximations due to their widespread implementation, and with Abedi and Stovas (2019a) because it has been introduced as the most accurate moveout approximation in VTI media. As Figure 5c shows, all the proposed approximations are more accurate than Alkhalifah and Tsvankin (1995); and the third and fourth-order approximations are more accurate than Fomel and Stovas (2010).

The accuracy of the proposed equations of the group direction as a function of phase direction, and vice versa, is shown in Figure 5d and 5e, respectively. The graphs show the difference between the exact and approximated angles in one domain, versus the corresponding angle in the other domain, which is very low.

The proposed kinematic approximations are made for homogeneous acoustic VTI media and, therefore, their accuracy comparison should be done in these media. However, in realistic subsurface models, which are at least vertically inhomogeneous, a moveout approximation that depends on three independent parameters is often used in velocity analysis and moveout correction. To study the effect of layering on fitting accuracy and parameter estimation by the proposed rational moveout approximations, we design another numerical study using another set of models that vary based on vertical inhomogeneity. We define ten models with the same depth and acquisition patterns, but with a varying number of layers from one to ten. All layers have fixed anisotropy parameters $\delta = -0.05,\ \eta = 0.3$, but defer based on the v_3 (vertical velocity of each layer) values. The vertical velocities in each layer of each model are defined so that t_0 of the reflection from the bottom of the model remains fixed. Figure 6a shows two representative models with five and ten layers, respectively. Figure 6b compares the maximum error of the best fit of different moveout approximations in each model. Figure 6c and Figure *6*d show the estimated effective model parameters resulted from each moveout approximation. For the one-layer model, the increase of accuracy from the second to the fourth order of our rational approximation can be seen in both the fitting accuracy and parameter estimation. However, adding the vertical inhomogeneity, the accuracy of different approximations becomes model dependent.

DISCUSSION

High accuracy and algebraic simplicity are two desirable aspects of an approximation. The algebraic simplicity of our approximations is due to their rational form. Rational equations are computationally efficient. In practice, this is important when an equation is calculated many times, such as the computation of phase velocity in seismic forward modeling algorithms, which is performed at each grid point. Using a Matlab program to compute the phase velocity at different angles for millions of homogenous models, we find that the computation time for our second- and third-order approximations are 35% and 43% of that for the exact equation, respectively.

The proposed approximations are highly accurate because of their matching internal symmetry with that of acoustic TI media, and the application of the optimal ray in parameter definition. We use the optimal ray in the definition of the approximations' parameters for three reasons: (1) The locations of the fittings become distributed at vertical, horizontal, and mid-angle directions, (2) A unique and simple definition is found for each parameter, and (3) The error of the first-order derivative of the approximation is kept low (because at all fitting directions we fit to exact kinematics and their derivatives). The latter is important in the phase-to-group, and group-to-phase conversions where the derivatives of equations should be accurate. The optimal ray direction is also the location of the maximum relative error in our approximations if all the parameters are defined at vertical and horizontal directions (Appendix B).

We propose different approximations for each kinematic properties because in selecting the maximum order of the continued fraction form in our approximations there is a tradeoff between the simplicity and higher accuracy. We have calculated the parameters up to an order of the general form that results in superior accuracy compared to the existing approximations.

We use the vertical and horizontal velocities to define the elliptical (or hyperbolic) backgrounds in our equations. This kind of parameterization is numerically shown to result in more accurate traveltime approximations (Xu and Stovas, 2016; Hao et al., 2019). While the definition of horizontal velocity for homogeneous media is evident and its conversion to NMO velocity is analytical, in layered media the horizontal velocity and its relation to NMO velocity are not clearly defined. The common definition is the Alkhalifah and Tsvankin (1995) approach to define the effective horizontal velocity as $V_{nmo}\sqrt{1+2\eta_e}$, where V_{nmo} and η_e are effective properties that are calculated by Dix averaging (e.g., equations 7 and 8 in Alkhalifah, 1997). Other definitions of the effective horizontal velocity are the Tsvankin and Thomsen (1994) approach to take the root mean square (RMS) of the horizontal velocities in layers, the Al-Dajani and Toksoz (2001) empirical approach to calculate the fourth-order averaging of the horizontal velocities, and the Ravve and Koren (2017) approach to use the maximum horizontal velocity in the overburden layers as the horizontal velocity for very large offsets. Although using the horizontal velocity to define the elliptical background is a better choice for homogeneous TI media, the finite offset ray-traced

parameterization for traveltime approximation in layered media becomes more complicated, because of the aforementioned problem with horizontal velocity definition.

CONCLUSION

We propose flexible functional equations for the approximation of P-wave kinematics in both phase and group domains, using a rational continued fraction form. Using different orders of the functional equations, we obtain different approximations that range from the simplest to the most accurate approximations. Therefore, a user can decide between the desired accuracy and algebraic simplicity of the approximations. Using the proper functional form and the robust parameter definition at the optimal ray, the proposed approximations, and their derivatives are highly accurate, as numerical tests on multiple models showed. However, in the group domain, we approximately reach the same level of accuracy of the phase domain, with one higher order of the continued fraction. We also propose the method of ray-traced parameter definition through a mid-angle or finite offset match, which extends the potential applications of our approximations to general 2D models. In the next part of this study, we will propose a 3D version of the rational approximations for P-wave kinematics.

ACKNOWLEDGEMENTS

I am grateful to the journal reviewers Igor Ravve, Vijay Singh, and an anonymous reviewer, and to the associate editor Ian Jones and the editor in chief Jeffrey Shragge for their insightful comments and suggestions. Gratitude is extended to David Pardo for helpful discussions. This work has received funding from the European Union's Horizon 2020 research and innovation programme under the grant agreement No 777778 (MATHROCKS), the European POCTEFA 2014-2020 Project PIXIL (EFA362/19) by the European Regional Development Fund (ERDF) through the Interreg V-A Spain-France-Andorra programme, the BCAM “Severo Ochoa” accreditation of excellence (SEV-2017-0718), the Basque Government through the BERC 2018-2021 program, and the grant "Artificial Intelligence in BCAM number EXP. 2019/00432".

DATA AND MATERIAL AVAILABILITY

Data and codes associated with this research are available and can be accessed at: https://www.mathworks.com/matlabcentral/fileexchange/75544-rational-approximation-of-p-wave-kinematics-part-i-vti

APPENDIX A

SERIES OF EXACT AND APPROXIMATED KINEMATICS

Here, we calculate the Taylor series expansion of the exact kinematics along the vertical (the first equation) and horizontal (the second equation) directions in equations A-1 to A-3:

$$
\begin{aligned}
v^2(n_1 \to 0, n_3) \approx{}& v_3^2 + \left(\frac{v_1^2}{1+2\eta} - v_3^2\right) n_1^2 + \frac{2\eta v_1^4 n_1^4}{v_3^2 (1+2\eta)^2} \\
&+ 2\eta v_1^4 \frac{(2\eta-1) v_1^2 + (1+2\eta) v_3^2}{(1+2\eta)^3 v_3^4} n_1^6 + \dots \\
v^2(n_1, n_3 \to 0) \approx{}& v_1^2 + \left(\frac{v_3^2}{1+2\eta} - v_1^2\right) n_3^2 + \frac{2\eta v_3^4 n_3^4}{v_1^2 (1+2\eta)^2} \\
&+ 2\eta v_3^4 \frac{(2\eta-1) v_3^2 + (1+2\eta) v_1^2}{(1+2\eta)^3 v_1^4} n_3^6 + \dots
\end{aligned}
\tag{A-1}
$$

$$
\begin{aligned}
V^2(N_1 \to 0, N_3) \approx{}& v_3^2 + \left(v_3^2 - \frac{(1+2\eta) v_3^4}{v_1^2}\right) N_1^2 + \left(v_3^2 - \frac{2(1+2\eta) v_3^4}{v_1^2} + \frac{(1+2\eta)^3 v_3^6}{v_1^4}\right) N_1^4 + \dots \\
V^2(N_1, N_3 \to 0) \approx{}& v_1^2 + \left(v_1^2 - \frac{(1+2\eta) v_1^4}{v_3^2}\right) N_3^2 + \left(v_1^2 - \frac{2(1+2\eta) v_1^4}{v_3^2} + \frac{(1+2\eta)^3 v_1^6}{v_3^4}\right) N_3^4 + \dots
\end{aligned}
\tag{A-2}
$$

$$
\begin{aligned}
t^2(x \to 0) \approx{}& t_0^2 + \frac{1+2\eta}{v_1^2} x^2 - \frac{2\eta(1+2\eta)^2}{t_0^2 v_1^4} x^4 + \frac{2\eta(1+2\eta)^3(1+6\eta)}{t_0^4 v_1^6} x^6 + \dots \\
t^2(x \to \infty) \approx{}& \frac{1}{v_1^2} x^2 + (1+2\eta) t_0^2 - 2\eta t_0^4 v_1^2 (1+2\eta)^2 x^{-2} \\
&+ \frac{1}{32}(1+2\eta)^3 \left(128\eta(1+2\eta(9+20\eta)) - 1\right) t_0^6 v_1^4 x^{-4} + \dots
\end{aligned}
\tag{A-3}
$$

We also calculate the Taylor series of the proposed approximations along the vertical and horizontal directions:

$$
\begin{aligned}
v^2(n_1 \to 0, n_3) \approx{}& v_3^2 + \left((1+A) v_1^2 - v_3^2\right) n_1^2 - \frac{A(1+B) v_1^4 n_1^4}{v_3^2} \\
&+ A \frac{(1+B(3+B+C)) v_1^6 - (1+B) v_1^4 v_3^2}{v_3^4} n_1^6 + \dots \\
v^2(n_1, n_3 \to 0) \approx{}& v_1^2 + \left((1+A) v_3^2 - v_1^2\right) n_3^2 - \frac{A(1+B) v_3^4 n_3^4}{v_1^2} \\
&+ A \frac{(1+B(3+B+C)) v_3^6 - (1+B) v_3^4 v_1^2}{v_1^4} n_3^6 + \dots
\end{aligned}
\tag{A-4}
$$

$$
\begin{aligned}
V^2\left(N_1 \to 0, N_3\right) \approx & v_3^2+\left(v_3^2-\frac{(1+A) v_3^4}{v_1^2}\right) N_1^2 \\
& +\left(v_3^2-\frac{2(1+A) v_3^4}{v_1^2}+\frac{\left(1+A\left(3+A+B\right)\right)^3 v_3^6}{v_1^4}\right) N_1^4+\ldots \\
V^2\left(N_1, N_3 \to 0\right) \approx & v_1^2+\left(v_1^2-\frac{(1+A) v_1^4}{v_3^2}\right) N_3^2 \\
& +\left(v_1^2-\frac{2(1+A) v_1^4}{v_3^2}+\frac{\left(1+A\left(3+A+B\right)\right)^3 v_1^6}{v_3^4}\right) N_3^4+\ldots
\end{aligned}
\tag{A-5}
$$

$$
\begin{aligned}
t^2\left(x \to 0\right) \approx & t_0^2+\frac{1+A}{v_1^2} x^2-\frac{A\left(1+B\right)}{t_0^2 v_1^4} x^4+A \frac{1+B\left(3+B+C\right)}{t_0^4 v_1^6} x^6+\ldots \\
t^2\left(x \to \infty\right) \approx & \frac{x^2}{v_1^2}+(1+A) t_0^2-A\left(1+B\right) t_0^4 v_1^2 x^{-2} \\
& +A\left(1+B\left(3+B+C\right)\right) t_0^6 v_1^4 x^{-4}+\ldots
\end{aligned}
\tag{A-6}
$$

The internal symmetry in these equations can be seen by comparing each term of the series expansions along vertical to the corresponding term along horizontal; their only difference is an interchange of the horizontal and vertical velocities. To more clearly see the symmetry in traveltime, t_0 should be replaced with z/v_3, where z is the depth of a diffraction or twice the depth of a reflector.

APPENDIX B

PROPERTIES OF OPTIMAL RAY

The proposed functional form of the approximations results in two fits to the exact kinematics through each parameter. For the first order of the general form in the phase domain (equation 3), the phase angle location of these dual fits (θ_a and θ_b) is obtained as,

$$
\sin\theta_a=\frac{u_1+u_2}{u_3},\ \sin\theta_b=\frac{u_1-u_2}{u_3},
\tag{B-1}
$$

where,

$$u_1 = v_1^2 v_3^2 \left(\left(1 + \left(1 + A \right)^2 \right) \left(1 + 2\eta \right) - 2 \right) - 2 v_3^4 \left(2\eta + A \left(1 + 2\eta \right) \right)$$
$$u_2 = A v_1^2 v_3^2 \sqrt{\left(2 + A \right)^2 \left(1 + 2\eta \right)^2 - 4 \left(1 + 2\eta \right)}, \tag{B-2}$$
$$u_3 = 2A^2 \left(1 + 2\eta \right) v_1^2 v_3^2 - 4\eta \left(v_1^2 - v_3^2 \right)^2 - 2A \left(1 + 2\eta \right) \left(v_1^2 - v_3^2 \right)^2 .$$

Finding A by matching the first-order approximation to the exact velocity along θ_a, it also gives the exact velocity along θ_b. The optimal ray directs to the center of this symmetrical dual fits that we get through each parameter of our approximations. Figure B-1 shows the relative error of equation 3 when parameter C is found by fitting equation 3 to the exact phase velocity along different directions, ranging from vertical to horizontal. The location of the fits is where the error graph reaches zero. Finding the location where these two fits meet, the direction of the optimal ray is calculated in the phase domain,

$$n_1 = \left(v_1 \sqrt{\frac{1}{v_1^2} + \frac{1}{v_3^2}} \right)^{-1}, n_3 = \left(v_3 \sqrt{\frac{1}{v_1^2} + \frac{1}{v_3^2}} \right)^{-1}, \tag{B-3}$$

and in the group domain,

$$N_1 = \frac{v_1}{\sqrt{v_1^2 + v_3^2}}, N_3 = \frac{v_3}{\sqrt{v_1^2 + v_3^2}}. \tag{B-4}$$

In Figure B-1 the darkest red line shows the error of equation 3 when C is obtained by fitting along the vertical and horizontal directions, and the darkest blue line shows the error when C is obtained by two fits in the optimal direction.

The corresponding exact phase velocity (v), group velocity (V), offset (x), traveltime (t), ray parameter (p), and curvature (Q) at the optimal ray are,

$$v^2 = \frac{v_1^2 v_3^2}{v_1^2 + v_3^2} \left(1 + \frac{1}{\sqrt{1 + 2\eta}} \right), \tag{B-5}$$

$$V^2 = \frac{1}{4} \left(v_1^2 + v_3^2 \right) \left(1 + \frac{1}{\sqrt{1 + 2\eta}} \right), \tag{B-6}$$

$$x = t_0 v_1, \tag{B-7}$$

$$t = 2t_0 \sqrt{\frac{\sqrt{1 + 2\eta}}{1 + \sqrt{1 + 2\eta}}}, \tag{B-8}$$

$$p = \left(v_1 \sqrt{1 + \frac{1}{\sqrt{1+2\eta}}} \right)^{-1}, \tag{B-9}$$

$$Q = -\left(2t_0 v_1 \sqrt{1 + 8\eta + \frac{1}{\sqrt{1+2\eta}}} \right)^{-1}. \tag{B-10}$$

The optimal ray is also the location of the maximum relative error in our approximations if all the parameters are defined in vertical and horizontal directions. This can be checked analytically (in phase domain), or numerically (in group domain), by taking the derivative of the relative errors at equations B-3 or B-4. The relative error is defined as,

$$RE_k = \left(\frac{k_{approximate} - k_{exact}}{k_{exact}} \right), \qquad \text{where } k = v, V, \text{or } t. \tag{B-11}$$

The relative error is multiplied by 100 to be in percent. The maximum relative errors of the second-order version of our approximations in equations 3, 7, and 11, when all the parameters are defined at vertical and horizontal directions are calculated as,

$$RE_v = 1 - 2\sqrt{\frac{(1+\eta)(1+2\eta)}{(2+3\eta)\left(1+2\eta+\sqrt{1+2\eta}\right)}}, \tag{B-12}$$

$$RE_V = -1 + 2\sqrt{\frac{\sqrt{1+2\eta}\left(1+\eta+\eta^2\right)}{\left(1+\sqrt{1+2\eta}\right)\left(2+3\eta+2\eta^2\right)}}, \tag{B-13}$$

$$RE_t = -1 + \sqrt{\frac{\left(1+\sqrt{1+2\eta}\right)\left(2+3\eta+2\eta^2\right)}{4\sqrt{1+2\eta}\left(1+\eta+\eta^2\right)}}. \tag{B-14}$$

Equation B-3, B-4, and B-7 show that the location of the maximum relative errors of proposed approximations is independent of anellipticity parameters; and equations B-12 to B-14 demonstrate that the magnitude of maximum relative errors depends solely on the anellipticity parameter.

REFERENCES

Abedi, M.M., and A. Stovas, 2019a, A new parameterization for generalized moveout approximation, based on three rays: Geophysical Prospecting, **67**, no.5, 1243-1255. DOI:10.1111/1365-2478.12770

Abedi, M.M., and A. Stovas, 2019b, Extended generalized nonhyperbolic moveout approximation: Geophysical Journal International, **216,** 1428-1440.

Abedi M.M., M.A. Riahi, and A. Stovas, 2019a, Three-parameter NMO correction in layered anisotropic media: a stretch-free approach: Geophysics, **84**, no. 3, C129–C142. DOI: 10.1190/geo2017-0855.1

Abedi M.M., M.A. Riahi, and A. Stovas, 2019b, Three-parameter Radon transform in layered transversely isotropic media: Geophysical Prospecting, **67,** 395–407.

Abedi, M.M., A. Stovas, and Y. Ivanov, 2019c, Acoustic wave propagation in orthorhombic media: phase velocity, group velocity, and moveout approximations: Geophysics, **84** no. 6, C269-C279.

Alashloo, S.Y.M., and D.P. Ghosh, 2018, Prestack depth imaging in complex structures using VTI fast marching traveltimes. Exploration Geophysics, **49** no.4, 484-493.

Al-Dajani A. and N. Toksoz. 2001, Non-hyperbolic Reflection Moveout for Orthorhombic Media: Earth Resources Laboratory, Department of Earth, Atmospheric, and Planetary Sciences, Massachusetts Institute of Technology, Cambridge, MA.

Aleixo R. and J. Schleicher, 2010, Traveltime approximations for qP waves in vertical transversely isotropy media: Geophysical Prospecting, **58** no. 2, 191-201.

Alkhalifah, T., 1997, Velocity analysis using nonhyperbolic moveout in transversely isotropic media: Geophysics, **62**, 1839-1854.

Alkhalifah T., 2000, The offset-midpoint traveltime pyramid in transversely isotropic media: Geophysics, **65**, 1316–25.

Alkhalifah T., 2011, Scanning anisotropy parameters in complex media: Geophysics **76**, no. 2, U13–22.

Alkhalifah T., and I. Tsvankin, 1995, Velocity analysis for transversely isotropic media: Geophysics, **60**, 1550-1566.

Eaton, D.W. S., 1993, Finite difference traveltime calculation for anisotropic media: Geophysical Journal International, **114**, 273–280, doi: 10.1111/j.1365-246X.1993.tb03915.x.

Fomel S., 2004, On anelliptic approximations for qP velocities in VTI media: Geophysical Prospecting, **52,** no.3, 247-259.

Fomel, S., and A. Stovas, 2010, Generalized nonhyperbolic moveout approximation: Geophysics, **75**, no. 2, U9-U18.

Fomel, S., L. Ying, and X. Song, 2013, Seismic wave extrapolation using lowrank symbol approximation: Geophysical Prospecting, **61**, 526–536. doi: 10.1111/j.1365-2478.2012.01064.x.

Hao, Q., bin U. Waheed, and T. Alkhalifah, 2019, P-wave complex-valued traveltimes in homogeneous attenuating transversely isotropic media. Geophysical Prospecting. **67** no. 9.

Muir F., and J. Dellinger, 1985, A practical anisotropic system: SEP **44**, 55–58. Stanford Exploration Project.

Pšenčík, I., B. Růžek, T. Lokajíček, and T. Svitek, 2018, Determination of rock-sample anisotropy from P-and S-wave traveltime inversion: Geophysical Journal International, **214**, 1088-1104.

Ristow, D., 1998, 3-D finite difference migration in azimuthally anisotropic media: 68th Annual International Meeting, SEG, Expanded Abstracts, 1823-1826.

Ravve I., and Z. Koren, 2017, Traveltime approximation in vertical transversely isotropic layered media, Geophysical Prospecting, **65** no.6, 1559-1581.

Song, H., Gao, Y., Zhang, J. and Yao, Z., 2016. Long-offset moveout for VTI using Padé approximation. Geophysics, **81** no.5, C219-C227.

Stovas A., and S. Fomel, 2017, The modified generalized moveout approximation: a new parameter selection: Geophysical Prospecting, **65** no. 3, 687-695.

Sripanich, Y., and S. Fomel, 2015, On anelliptic approximations for qP velocities in transversely isotropic and orthorhombic media: Geophysics, **80** no. 5, C89–C105, doi: 10.1190/geo2014-0534.1.

Stovas, A., and S. Fomel, 2019, Generalized velocity approximation: Geophysics, **84** no. 1, C27-C40.

Stovas, A., Y. Roganov, and V. Roganov, 2018, Difference between phase and group angles in ORT media: In 17th International Conference on Geoinformatics-Theoretical and Applied Aspects. EAGE, 12510_ENG.

Thomsen, L., 1986, Weak elastic anisotropy: Geophysics, **51**, 1954-1966.

Tsvankin I., and L. Thomsen, 1994, Nonhyperbolic reflection moveout in anisotropic media: Geophysics, **59**, 1290-1304.

Ursin B., and A. Stovas, 2006, Traveltime approximations for a layered transversely isotropic medium. Geophysics, **71** no.2, D23–33.

Xu, S. and A. Stovas, 2017, A new parameterization for acoustic orthorhombic: Geophysics, **82** no. 6, C229-C240.

Xu, S., A. Stovas, and Q., Hao, 2017, Perturbation-based moveout approximations in anisotropic media: Geophysical Prospecting, **65**, no.5, 1218-1230.

List of Figures

Table 1. The types of fits of the proposed approximations to the exact kinematics. The table shows what properties of the proposed equations are exact in each direction. Superscript numbers show the order of derivative (the negative value shows antiderivative). The exact properties at vertical and horizontal directions can be found in the series terms in Appendix A, and the exact properties at the optimal direction can be found in Appendix B.

	At vertical	**At optimal**	**At horizontal**
Equation 3, 2nd order	$v_3, v^{(2)}$	$v, v^{(1)}$	$v_1, v^{(2)}$
Equation 3, 3rd order	$v_3, v^{(2)}, v^{(4)}$	$v, v^{(1)}$	$v_1, v^{(2)}, v^{(4)}$
Equation 7, 2nd order	$v_3, V^{(2)}$	$V, V^{(1)}$	$v_1, V^{(2)}$
Equation 7, 3rd order	$v_3, V^{(2)}, V^{(4)}$	$V, V^{(1)}$	$v_1, V^{(2)}, V^{(4)}$
Equation 7, 4th order	$v_3, V^{(2)}, V^{(4)}$	$V, V^{(1)}, V^{(2)}, V^{(3)}$	$v_1, V^{(2)}, V^{(4)}$
Equation 11, 2nd order	t_0, v_{nmo}	t, p	v_1, t
Equation 11, 3rd order	t_0, v_{nmo}, η	t, p	$v_1, t, t^{(-2)}$
Equation 11, 4th order	t_0, v_{nmo}, η	$t, p, Q, t^{(3)}$	$v_1, t, t^{(-2)}$

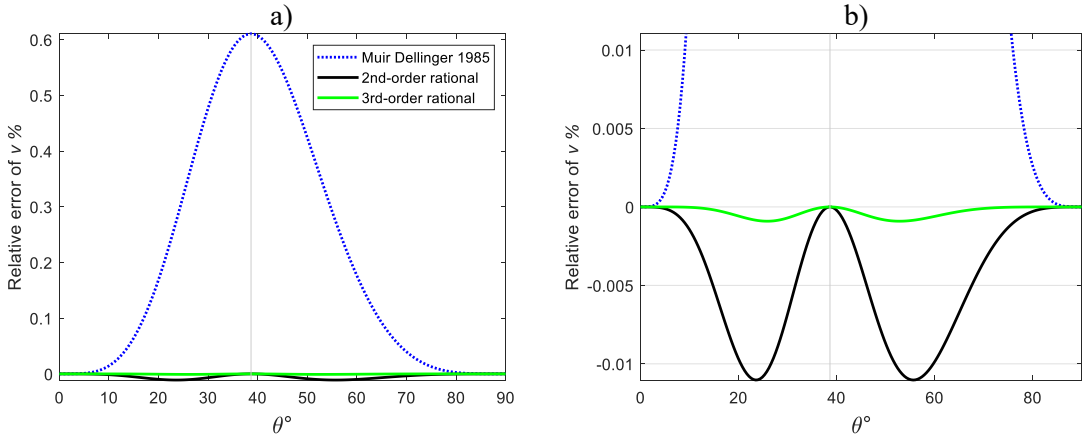

Figure 1. (a) Relative errors of different phase velocity approximations, using an acoustic VTI model with $\eta = 0.3$. The second, and third-order of our approximation are obtained by inserting equations 4, and 5, into equation 3, respectively. (b) The same graphs as the left panel, but with a finer vertical scale. In this and the following figures, a vertical gray line shows the direction of the optimal ray.

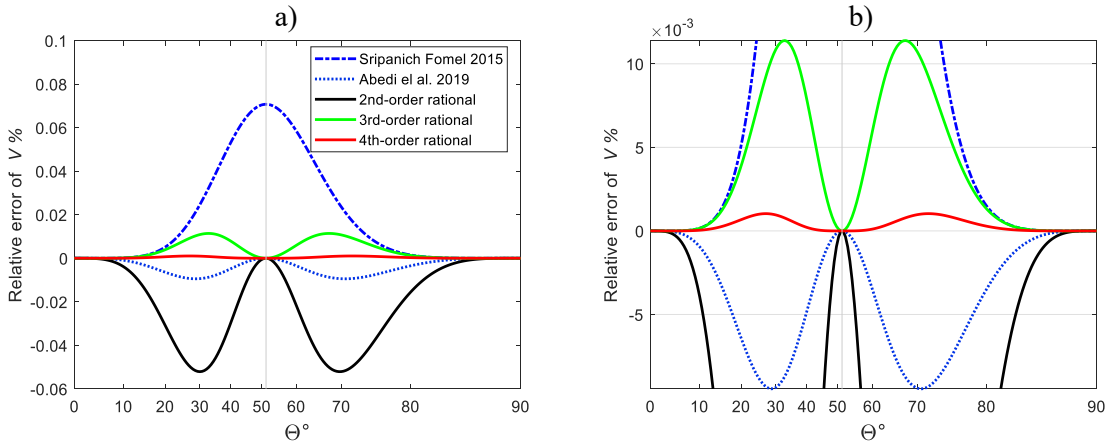

Figure 2. (a) Relative errors of different group velocity approximations. The model is defined in Figure 1. The second, third, and fourth-order of our approximation are obtained by inserting equations 8, 9, 10, into equation 7, respectively. (b) The same graphs but in different vertical scales. Note that the horizontal axis is kept linear in terms of the phase angle.

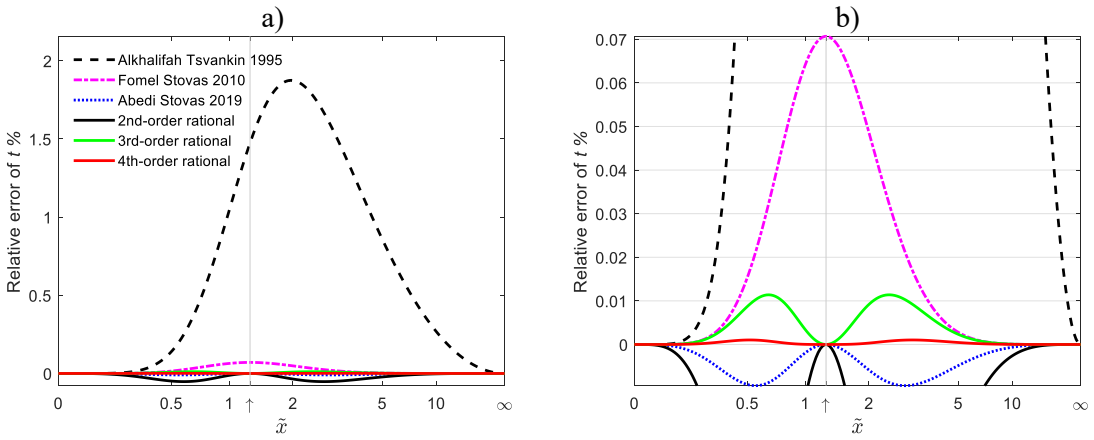

Figure 3. The same as the previous figure, but for traveltime versus normalized offset.

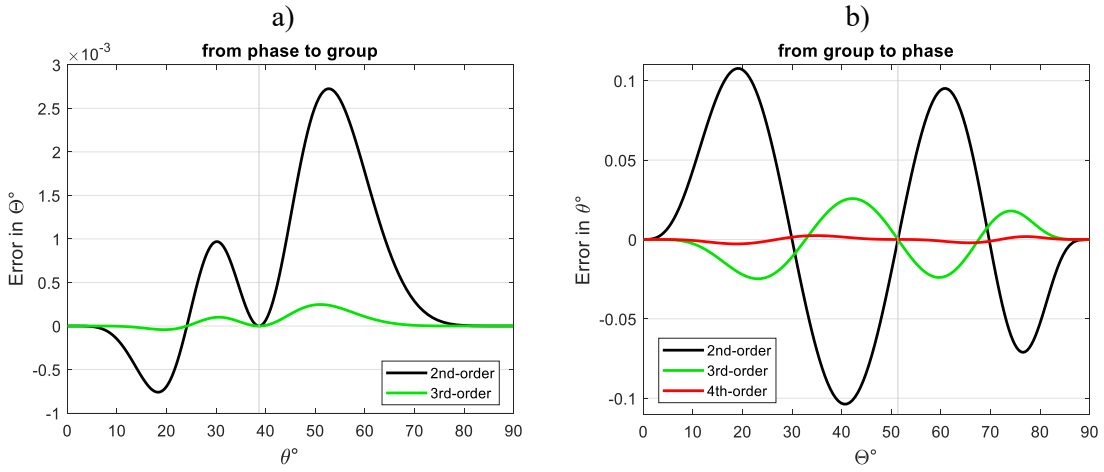

Figure 4. (a) The error in the approximation of group direction as a function of phase direction (equation 12). (b) The error in phase direction as a function of group direction (equation 14), using an acoustic VTI model with $\eta = 0.3$.

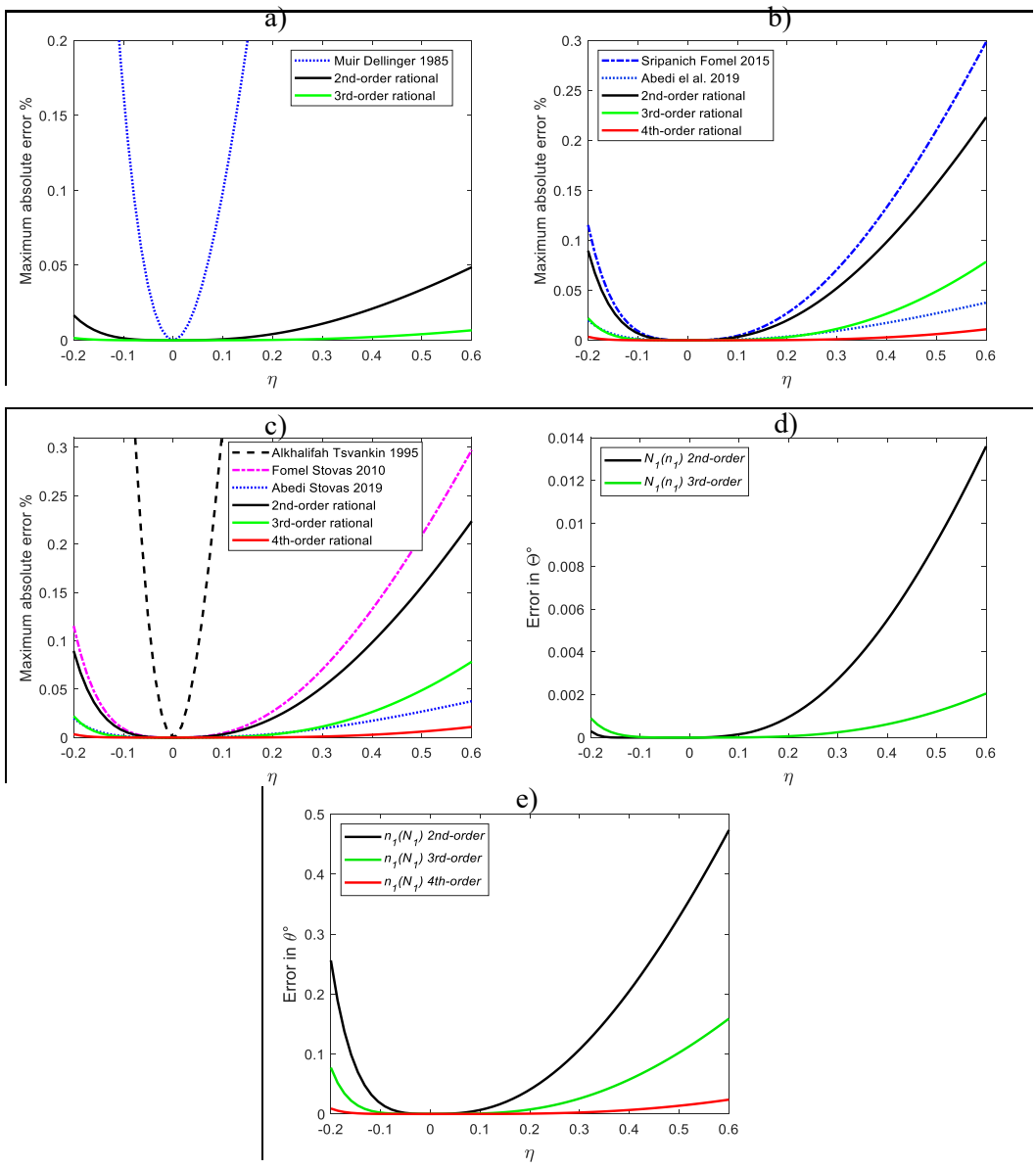

Figure 5. Comparison of the maximum magnitude errors of different kinematic approximations, using multiple models with different anellipticity parameters. a) Approximations of phase velocity, b) group velocity, c) traveltime, d) phase-to-group and, e) group-to-phase direction conversions.

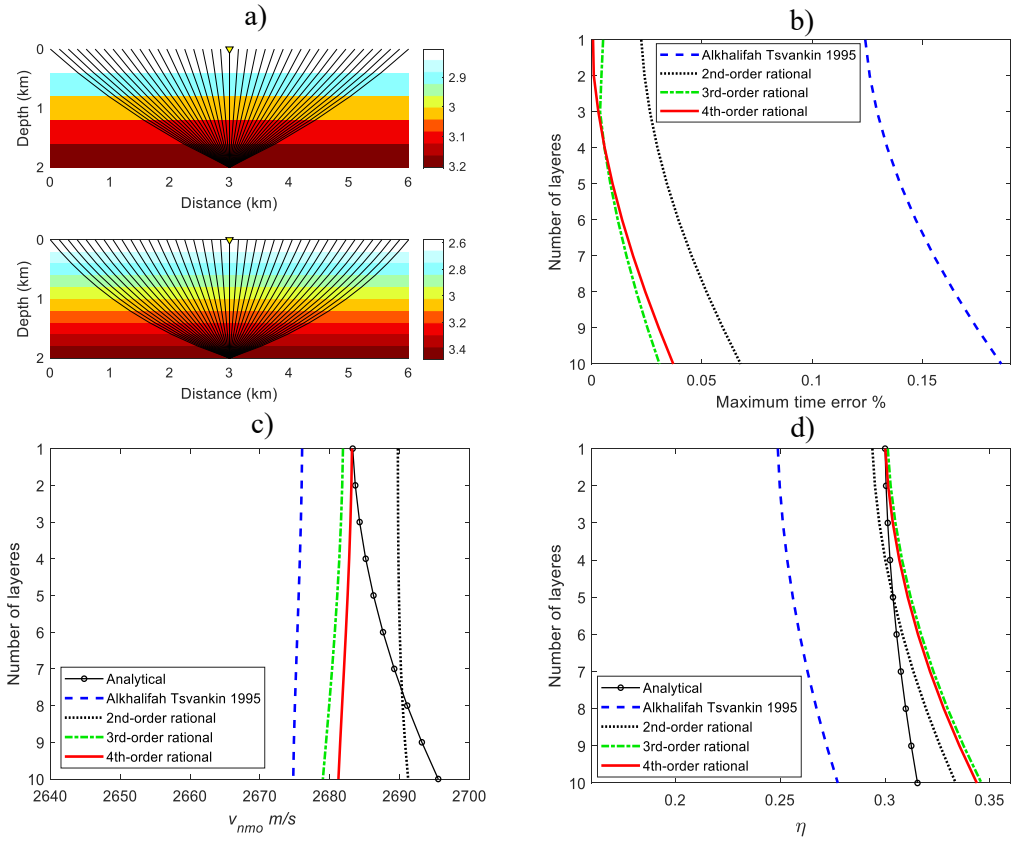

Figure 6. A numerical experiment for evaluating the performance of the proposed moveout approximations in vertically layered media. a) Two representatives of ten models that have a different number of layering, but fixed reflector depth and acquisition patterns (color bars show v_3 in km/s). b) The maximum relative errors of the best fit of each moveout approximation to the ray-traced traveltimes. c) Estimated effective NMO velocity, and d) estimated effective anellipticity from each equation.

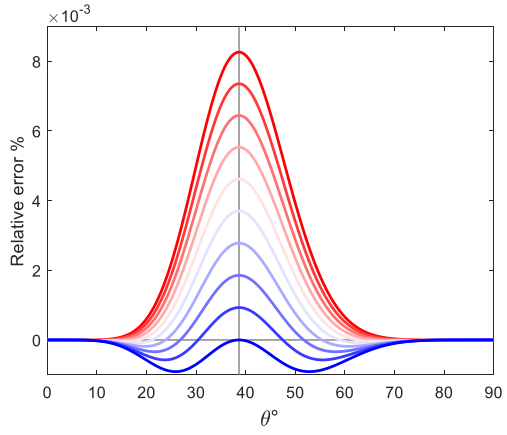

Figure B-1. The relative error of equation 3 for different definitions of parameter *C*. From the dark red to the dark blue line, the fitting direction is changed from vertical (and horizontal) to the optimal. The vertical gray line shows the direction of the optimal ray. The location of fits is where the error reaches zero.